Short Papers

Efficient Lane Detection Based on Spatiotemporal Images

Soonhong Jung, Junsic Youn, and Sanghoon Sull, *Senior Member, IEEE*

***Abstract*—In this paper, we propose an efficient method for reliably detecting road lanes based on spatiotemporal images. In an aligned spatiotemporal image generated by accumulating the pixels on a scanline along the time axis and aligning consecutive scanlines, the trajectory of the lane points appears smooth and forms a straight line. The aligned spatiotemporal image is binarized, and two dominant parallel straight lines resulting from the temporal consistency of lane width on a given scanline are detected using a Hough transform, reducing alignment errors. The left and right lane points are then detected near the intersections of the straight lines and the current scanline. Our spatiotemporal domain approach is more robust missing or occluded lanes than existing frame-based approaches. Furthermore, the experimental results show not only computation times reduced to as little as one-third but also a slightly improved rate of detection.**

***Index Terms*—Spatiotemporal image, scanline, temporal consistency, lane detection, alignment, binarization, Hough transform, lane tracking, cubic model.**

I. Introduction

Smart driving assistance systems are becoming increasingly popular with the introduction of applications such as lane departure warnings [1] and road marking identification [2]. These applications, and others like them, require the efficient detection of the lanes on a road; however, reliably detecting those lanes using input video remains challenging in situations where they are not clearly visible, such as when there are missing lane markings or lane-like noise. Therefore, developing an efficient and reliable lane detection method remains a priority.

Existing lane detection methods generally consist of two main steps: detecting lanes and fitting them to a parametric curve. To detect lanes, a color frame image is first converted into a gray-level one by generating a luminance image [3]–[9], or a fixed RGB ratio image for yellow lane markings [10]. A gradient-enhancing image has also been used which maximizes the gradient between road and the lane marking color values [11]. In [12], histogram equalization is adopted to enhance low contrast images. To transform an input image into a binary one, an edge-based gradient operator such as a Canny edge detector [3], [4], [11], [12], [26], [27], a Sobel edge detector [5] or an adaptive threshold [9] is used. Steerable filters [13], [16], Gaussian filters [6], mean/weighted filters [8], adaptive threshold filters [9], and filters based on gradient values [14], [28] have also been used to enhance lane-like edges and reduce noise. Some approaches use the color value differences between the road and lane markings using empirical thresholding [17] and fuzzy c-means clustering [18]. In [19], a learning approach using edge and texture features is suggested.

For the detection of curving lanes, the detected lane points need to be fit on a curve. Curving lanes are usually represented by the complex clothoid curving model [20], [21]. Thus, many algorithms use an approximated clothoid model, such as cubic curve [12], [22], quadratic curve [11], straight line [9], [26], [28] B-spline [3], hyperbola [4], pairwise hyperbola [7], and mixed polynomial curve [10] models.

Existing approaches have difficulty detecting lanes which are noisy or not clearly visible. Edge-based approaches [3]–[16] are rendered less accurate by lane-like noise caused by the lens flare effect, while color-based approaches [17], [18] are sensitive to changes in illumination. Most methods [3]–[22], [26]–[28] also struggle to detect and track lanes that are missing some sections. Although the use of motion vectors or optical flow [23] can be used to avoid these complications, they require higher computational power, and motion vectors cannot be reliably computed for sections of road that do not have texture.

Our approach is based on the observation that the lane width on a horizontal scanline is consistently uniform along the time axis over a succession of frames or, put another way, the lane width on the scanline has temporal consistency, because the position and orientation of the camera with respect to the road does not change greatly. In this paper, we use spatiotemporal images [24], [25] generated by accumulating a set of pixels sampled at a horizontal scanline consistently located on each frame along a time axis. In a spatiotemporal image, if consecutive scanlines are aligned, the trajectory of the lane points is readily visible and appears as two dominant parallel straight lines due to the temporal consistency. Thus, by detecting those two dominant parallel lines, lane points can be reliably and efficiently detected.

In this paper, we propose an efficient method for reliably detecting and tracking lanes using spatiotemporal images. For a given scanline frame position, after a spatiotemporal image has been constructed, consecutive scanlines are aligned for a given period of time (120 frames, for example), yielding two parallel lines due to the temporal consistency. Although the alignment of two consecutive scanlines is usually inexact due to road markings and occluded lanes, the alignment of multiple consecutive scanlines along the time axis is likely to produce a predominantly straight line. The scanlines in each spatiotemporal image are then more finely aligned as follows: 1) the spatiotemporal image is binarized, changing the brighter pixels into white pixels; 2) two dominant parallel straight lines are detected by applying a Hough transform to the binarized image; and 3) each lane point is detected by selecting the center pixel of the connected white pixel block nearest to the intersection point of the dominant straight line and the scanline. An offset value used to align the scanline in the next frame is predicted by the detected lane points. When all scanlines have been processed, the detected lane points are fitted to a cubic model using a weighted least squares algorithm. Our method is more efficient due to using only a fraction of a frame and robust to missing lane due to its use of multiple frames when detecting lane points.

Manuscript received July 6, 2014; revised January 27, 2015 and June 1, 2015; accepted July 28, 2015. Date of publication August 21, 2015; date of current version December 24, 2015. This work was supported by the Basic Science Research Program through the National Research Foundation of Korea funded by the Ministry of Education (NRF-2012R1A1A2044892). The Associate Editor for this paper was S. S. Nedevschi.

The authors are with the School of Electrical Engineering, Korea University, Seoul 136-701, Korea (e-mail: shjung@mpeg.korea.ac.kr; jsyoun@mpeg.korea.ac.kr; sull@korea.ac.kr).

Color versions of one or more of the figures in this paper are available online at http://ieeexplore.ieee.org.

Digital Object Identifier 10.1109/TITS.2015.2464253

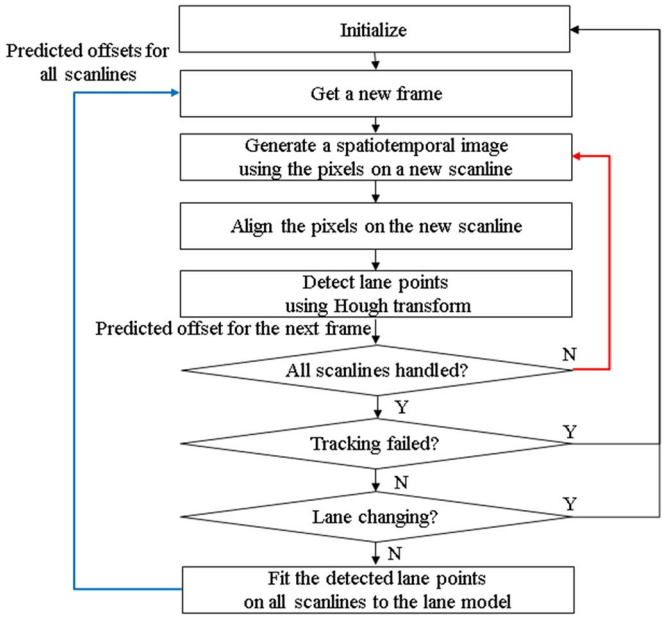

Fig. 1. Overall process of the proposed method.

This paper is organized as follows. In Section II, we describe the proposed algorithm. In Section III, we present the experimental results. Finally, in Section IV we conclude the paper.

II. Proposed Method

In this section, we describe the details of the proposed lane detection method; the overall process is shown in Fig. 1, where the blue outer loop and the red inner loop are repeated for each frame and each scanline, respectively. We also explain how our algorithm handles four complicating factors, lane changes, speed bumps, lens flares, and missing lanes.

A. Generation of Spatiotemporal Images

Each frame from an input video filmed by a vehicle-mounted camera is converted to a gray-level image using the color ratio in [10]. K spatiotemporal images are then generated from the video. Each spatiotemporal image is obtained by accumulating a set of pixel lines, sampled from a constant location on each successive frame, along a time axis [24], [25]. Let $I(x, y, t)$ be the pixel value at location (x, y) and time t in the video. Then, from the video volume shown in Fig. 2(a), the $x-t$ spatiotemporal image sampled at the scanline $y = y_k$ can be expressed as

$$I_{ST}(x,\ t) = I(x, y_k, t). \tag{1}$$

The size of the spatiotemporal image is $X \times T$, where X and T are the width and the duration of the video volume, respectively. For the real-time detection of lane points, we only use sampled pixels on scanlines from the current time t_c to $t_c - t_p + 1$, where t_p is set to 4 seconds. More than four horizontal pixel sampling schemes or scanlines are used because at least four points are required to fit a cubic curve model and thereby produce a smooth representation within the video frame. The scanlines in an individual frame and the spatiotemporal images constructed at the scanlines $y = y_1$ and $y = y_3$ are shown in Fig. 2. In the spatiotemporal image, lane widths look uniform because the distance from the camera to the lane is also usually uniform. Note that, in Fig. 2(b) and (c), the lane points in the spatiotemporal images become clearly visible without the need for further processing, such as by Inversed Perspective Mapping (IPM) [9].

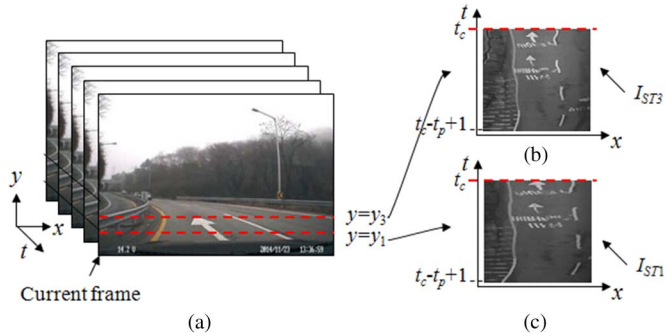

Fig. 2. An example of the generation of spatiotemporal images. (a) The position of the scanlines. (b)–(c) Spatiotemporal images from current time t_c to $t_c - t_p + 1$ at scanlines $y = y_3$, and y_1, respectively.

B. Alignment of Spatiotemporal Images

The trajectories of the lane points in the spatiotemporal images in Fig. 2(b) and (c) appear smooth when the vehicle is driven normally between the left and right lane markings. The lane points in the spatiotemporal images also generally look brighter on darker backgrounds. Further, our process uses the temporal consistency of the lane width on each scanline, or to be more explicit, it uses the fact that the lane width on constantly located horizontal scanlines is consistent between frames along the time axis because the position and orientation of the camera does not change greatly with respect to the road. Thus, it is likely that the lane points between consecutive scanlines will be aligned, resulting in two parallel lines. To align two consecutive scanlines, simple motion compensation along the x-axis is performed using the gradient difference between consecutive scanlines in order to be robust to changes in illumination. For the alignment, the following offset function $O(t)$ is first computed:

$$O(t) = \underset{k \in [-w_R, w_R]}{\arg\min}\ \mathrm{SAD}(k, t) \tag{2}$$

where the integer k is a search distance for the compensation (or alignment) that ranges between $-w_R$ and $+w_R$ and $\mathrm{SAD}(k,\ t)$ is the sum of the absolute difference of the gradient values between consecutive scanlines at t and $t-1$ when the scanline at t is shifted by k. In the initialization step of our algorithm, all pixels on one scanline are used to calculate SAD. However, once predicted lane points become available later, a connected subset of pixels that sufficiently cover the predicted left and right lane points on the scanline are used to compute SAD. If the minimum value of $\mathrm{SAD}(O(t_c), t_c)$ for the current scanline at $t = t_c$ is larger than the threshold value T_d, the $O(t_c)$ is set to the predicted offset of the previous frame. The search range w_R is also determined by the predicted lane points using a Hough transform, as will be explained in Section II-C. The aligned spatiotemporal image $I_A(x,\ t)$ at $t = t_c$ is then generated by incrementally shifting the scanline by the computed offset as follows:

$$I_A(x, t_c) = I_{ST}\left(x - \sum_{t=t_i}^{t_c} O(t), t_c\right) \tag{3}$$

where t_i is the time of the initialization step.

Fig. 3 shows the offset function for the spatiotemporal image in Fig. 2(c) and the resulting aligned spatiotemporal image. The trajectories of the lane points in the aligned spatiotemporal image become

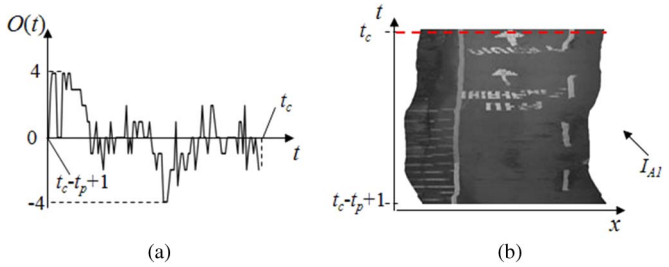

Fig. 3. Aligning a spatiotemporal image. (a) An offset function for the spatiotemporal image in Fig. 2(c). (b) The aligned version of the spatiotemporal image from Fig. 2(c).

predominantly parallel straight lines which are easier to detect in the next step.

C. Detection of Lane Points in Aligned Spatiotemporal Images

In the alignment step, the lane points between consecutive scanlines were aligned, resulting in two parallel lines. Although the alignment of two consecutive scanlines is usually not exact due to road markings, occluded lanes, skid marks, and other impediments, the alignment of multiple consecutive scanlines along the time axis is likely to produce a predominantly straight line. First, because the distribution of the pixel values of the lanes on a road and their boundaries can be modeled as a Gaussian function, a two-dimensional Gaussian filter with a Gaussian kernel of size 11×11 and an adaptive threshold [6] is used to construct a binary image of the aligned spatiotemporal image. Next, a morphology operation, such as opening and closing, is applied to the binary image.

The two primarily parallel straight lines that are likely to correspond to the lane points are detected by applying a Hough transform to the binary image. The slope of the straight line for the Hough transform is set to 80°–100° to make up for slight alignment errors. The lane points on each scanline are detected by selecting the center pixel of the connected white pixel block nearest to the intersection point of the dominant straight line and the current scanline as shown in Fig. 4(b). The detected lane points can then be marked in the frame by adding the value of $O(t_c)$, as shown in Fig. 4(c). The offset value used to align the scanline in the next frame is predicted by the detected lane points. When no nearby connected white pixel block is found due to a missing lane marking, it is predicted by the intersection of the Hough line and the current scanline. If the two lane points are missing completely, they can be still be approximated by using the offset predicted in the previous frame. If the lane markings are completely missing or not visible for an extended period of time, such as that corresponding to 60 frames, the algorithm is reinitialized and restarted.

D. Lane Fitting

For the detection of lane points for curving lanes, a clothoid curving model [20], [21] can be employed. It is defined by its beginning curvature, a constant curvature change rate and its total length. In this paper, we use a simple cubic model to fit the lane. Although the cubic model with four parameters requires at least four lane points for each lane to calculate its parameters, for reliability we fit seven detected lane points from the corresponding scanlines ($K = 7$) into a cubic model by using a weighted least square fitting method. A weight of 0.75 is given to detected lane points corresponding to the center pixel of the white pixel block nearest along the current scanline to the intersection of the scanline and the dominant straight line. On the other hand, a weight of 0.25 is given to less reliable detected lane points, predicted only from the intersection because there are no nearby connected white pixel blocks. If more complex lanes are present on the road, the proposed algorithm is easily extended by using additional scanlines at the expense of more computation.

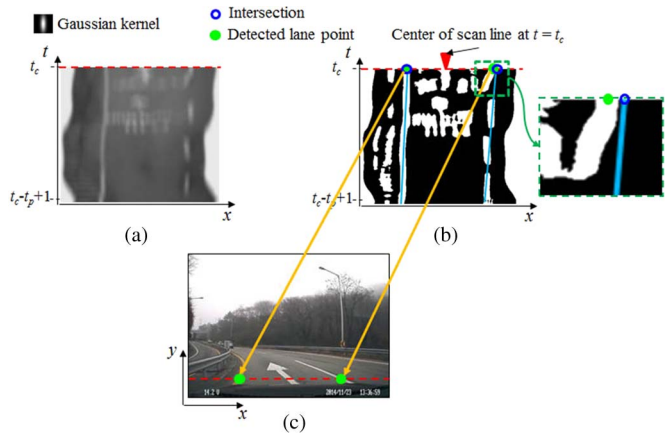

Fig. 4. Detection of lane points in a binary image. The blue solid lines indicate the results of a Hough transform. The blue circles indicate the intersection between the current scanline and the parallel straight lines, and the green circles the intersection between the current scanline and the detected lane point nearest to the intersection. (a) A kernel image for a 2D Gaussian filter and filtered images from I_{A1} in Fig. 3(b). (b) The binary image obtained from (a) and a magnified view of a dashed rectangular box. (c) The corresponding frame at $t = t_c$.

Fig. 5. Result of fitting a lane to a cubic model using weighted least squares. The green and blue circles indicate the detected lane points and a predicted lane point, respectively.

Fig. 5 shows the results of lane detection after the data is fitted to the cubic model; the green and blue circles indicate the detected lane points and one predicted lane point, respectively.

E. Abnormal Cases

In this subsection, we describe the management of four abnormal cases: lane changes, speed bumps, lens flares, and missing lanes.

1) Changing Lanes: If a driver changes lanes, the trajectory of lane points appears slanted or curved (Fig. 6). The spatiotemporal image in Fig. 6(a) is transformed into an aligned spatiotemporal image in Fig. 6(b) so that the lane points become aligned in a straight line despite the trajectory of the lane points being slanted during the lane change intervals (I_a and I_b). Fig. 6(c) shows the result of detecting lane points using a Hough transform; it can be seen that the lane change is reliably detected by comparing the lane points with the center of the scanline.

2) Speed Bumps: If the road is not flat, existing methods (such as those in [9] and [11]) fail to detect lanes due to abrupt changes in their orientation with respect to the camera and a change in the region of

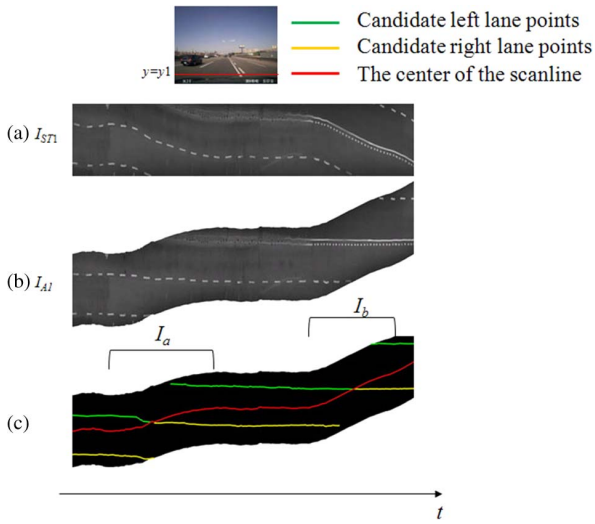

Fig. 6. An example of a lane change. (a) The spatiotemporal image. (b) The aligned spatiotemporal image. (c) The result of lane point detection using a Hough transform.

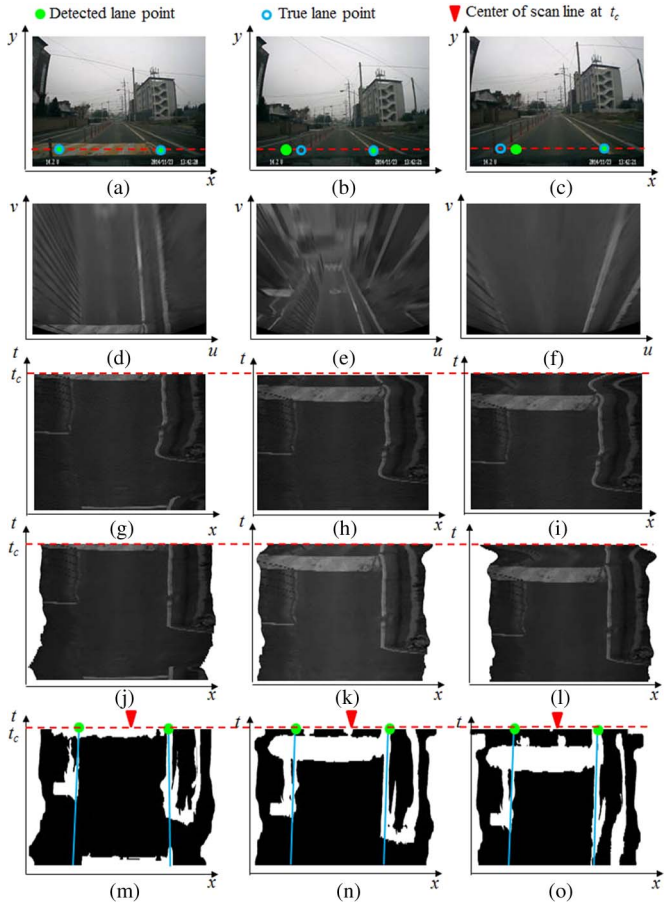

Fig. 7. An example of a speed bump. The first, second, and third columns indicate the normal, jumping over, and jumping down cases of the vehicle, respectively. (a)–(c) Input frames. (d)–(f) IPM images from the input frames. (g)–(i) Spatiotemporal images. (j)–(l) Aligned spatiotemporal images. (m)–(o) Binary images.

interest (ROI). For a speed bump video sequence with severe pitch angle variation where the left lane markings are not clearly visible, only the right lane points are correctly detected and aligned, but the left lane points predicted from the previous frame show some error

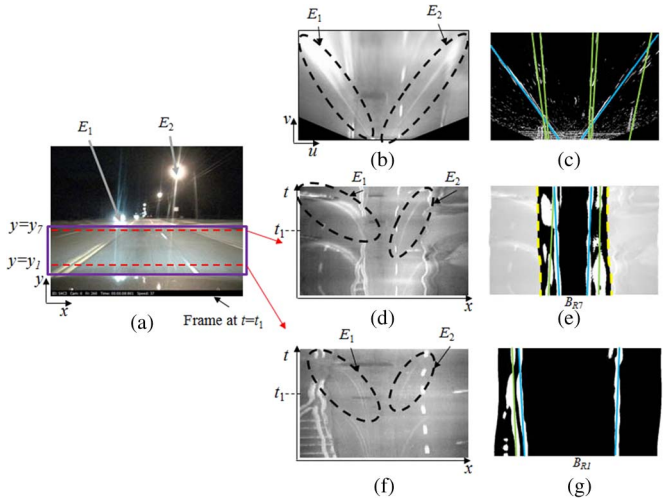

Fig. 8. An example of the lens flare effect. E_1 and E_2 are lens flares caused by a vehicle and street lights, respectively. (a) The original frame where the red dashed lines indicate the scanlines used to generate the spatiotemporal images and the purple solid box indicates the ROI for an IPM image. (b)–(c) An IPM frame image and its binary image with the incorrect result of a Hough transform (blue lines) using the method in [9]. (d)–(g) Spatiotemporal images at the scanlines ($y = y_7$ and $y = y_1$) and their binary images with the correct results of a Hough transform (blue lines) using the proposed method. Only the pixels surrounded by the yellow dashed line are used to compute the offset function.

because the width of the lane abruptly changes in the spatiotemporal image as shown in Fig. 7(k)–(l). However, our algorithm continues to function as soon as the speed bump is passed over. When both lanes are clearly visible or the pitch angle variation is not severe, our algorithm works correctly by selecting the center pixel of the connected white pixel block nearest along the current scanline to the intersection of the scanline with the Hough line (Fig. 4). It should be noted that the orientation of lanes in the IPM image is very sensitive to pitch angle variation as shown in Fig. 7(e)–(f).

3) Lens Flares: It is sometimes difficult to reliably detect lanes or lane points due to the lens flare effect caused by the lights of other vehicles (E_1) or street lamps (E_2) as shown in Fig. 8. In the spatiotemporal images in Fig. 8(d) and (f), the lens flares appear as curved lines and remain so after aligning the spatiotemporal image. Thus, our algorithm can correctly detect the lane points by detecting two parallel straight lines using a Hough transform as shown in Fig. 8(e) and (g). However, as shown in Fig. 8(c), Borkar's method [9] yields an incorrect result since it detects dominant lines using a Hough transform in the IPM image. In Fig. 8(e), only the pixels surrounded by the yellow dashed line sufficiently covering the predicted left and right lane points on the scanline are used to calculate the offset function.

4) Missing Lanes: Fig. 9 shows an example of tracking lane markings that are missing on one side of the lane due to faded paint, indicated by the green dashed line. If the left and the right lanes are tracked independently as in [9], the result is unsatisfactory as shown by the incorrectly detected right lane in Fig. 9(b). However, in the proposed method, the missing lane points can be predicted accurately by the intersection of the Hough line and the current scanline even when the vehicle is moving slightly left or right because the scanline can be aligned by considering the temporal consistency of lane width in the spatiotemporal image.

Fig. 10 depicts a lane that is partially occluded in the presence of an obstacle such as another vehicle. Using alignment, binarization and a Hough transform, the proposed method is still able to reliably detect the lane even though the aligned spatiotemporal image is imperfect.

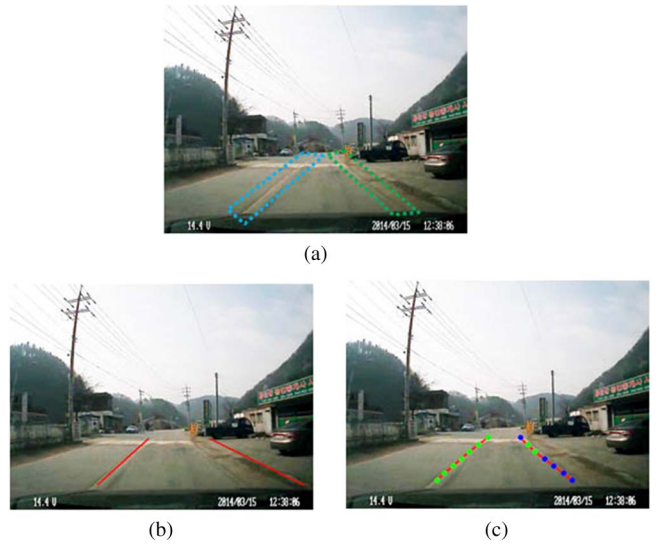

Fig. 9. An example of tracking a missing lane. (a) The original frame with the regions containing the lane markings and missing lane markings (the blue and green dashed lines, respectively). (b) The result using the method in [9]. (c) The result using the proposed method.

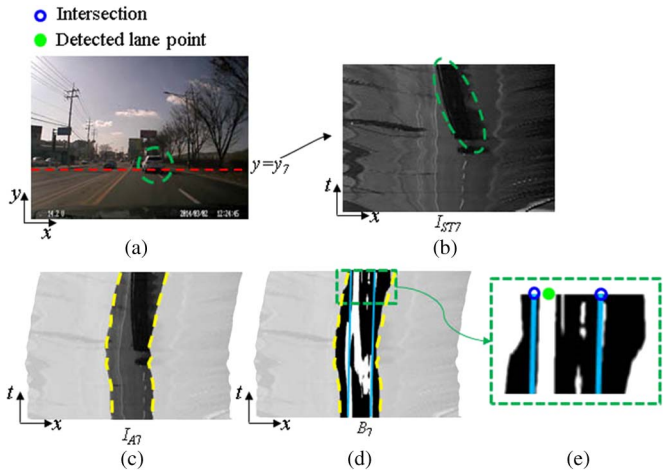

Fig. 10. An example of the presence of obstacles. The green dashed circle indicates an obstacle. Only the pixels surrounded by the yellow dashed line are used to compute the offset function. (a) The original frame including the obstacle. (b) The spatiotemporal image at scanline $y = y_7$. (c) The aligned spatiotemporal image. (d) The binary image with the results of a Hough transform (blue solid line). (e) The magnified view including the intersection between the current scanline and the parallel straight line, and a detected lane point.

Although there is no candidate right lane point as shown in Fig. 10(e), the lane point can be tracked by the intersection of the Hough line and the current scanline. However, when both the left and right lanes are completely occluded by obstacles, the proposed method and the existing methods of [9] and [11] fail to detect the lane. If the lanes are completely missing or not visible for a certain period of time, the algorithm is reinitialized and restarted.

III. Experimental Results

The performance of the proposed system was evaluated on a PC with a 2.8 GHz CPU and 4 GB of RAM. Two existing methods (Borkar [9] and Yoo [11]) were tested alongside the proposed approach for their lane detection performance. Borkar's method [9] generates ground truth data by manually detecting the lane points in a spatiotemporal image and interpolating the lane points, and it detects lanes based on a frame rather than a spatiotemporal image. Yoo's method [11] detects lanes using an adaptive Canny edge detector on the gradient-enhancing image also based on a frame. Three datasets were used as the basis of the comparison (Borkar [9], Yoo [11], and our dataset).

TABLE I
Lane Detection Rate for Dataset [9]

Category	Borkar [9]	**Proposed**
Isolated Highway	98.24%	**98.31%**
Metro Highway	98.12%	**98.33%**
City	87.21%	**90.52%**

TABLE II
Lane Detection Rate for Dataset [11]

	Aly [6]	Borkar [9]	Yoo [11]	**Proposed**
Average	72.94%	81.53%	96.37%	**97.68%**

TABLE III
Lane Detection Rate for our Dataset

Category	Borkar [9]	Yoo [11]	**Proposed**
Highway	97.10%	95.34%	**98.21%**
City	82.67%	83.27%	**87.64%**
City at night	79.22%	85.76%	**87.67%**
Country	59.20%	64.12%	**79.60%**
Average	79.61%	82.30%	**88.70%**

Our video dataset, taken by a vehicle mounted camera located behind the rear-view mirror and totaling 1 hour 40 minutes at 640 × 480, included four road categories, highway, city, city-night, and country. The ground truth was manually generated by us.

Table I presents the lane detection results when applying Borkar's method and then the proposed method to Borkar's dataset [9]. The proposed method demonstrated better results, especially for video taken in the city which often contained missing lanes and lens flare, because Borkar's method does not consider spatiotemporal consistency but rather analyzes each frame separately.

Table II shows the results of lane detection using the proposed method and three existing methods [6], [9], and [11] with Yoo's dataset [11], which covers various environments such as night-lamp, rain, and route-sunset. Yoo's method is robust for these environments because it maximizes the gradient between the road and its lane color. However, it sometimes yields erroneous results due to its enhancement of lane-like noise. Overall, the proposed method yields satisfactory results.

Table III and Fig. 11 present the lane detection results for two existing methods [9], [11] and the proposed method with our dataset. Yoo's method demonstrated a lower performance with videos shot in the highway during the day due to its enhancement of lane-like noise. Borkar's method had some difficulty detecting lanes with videos shot in the city because they were not clearly visible, especially at night. All three methods yield lower performance with videos shot in the country which contain several abnormal cases such as speed bumps and missing lanes. In the speed bump, Borkar's and Yoo's methods fail

Fig. 11. Results of the proposed method and the two existing methods [9] and [11] for our dataset. (a) Borkar [9]. (b) Yoo [11]. (c) Proposed method.

to detect lanes due to abrupt changes in their orientation with respect to the camera and a change in the ROI, respectively. The proposed method also exhibits some error because the width of the lane abruptly changes in the spatiotemporal image due to the pitch angle variations and thus violates the temporal consistency assumption. As soon the speed bumps are passed, however, both lane points are successfully detected once more. When either of the left or the right lane (but not both) is completely missing, the proposed method can detect lanes by using the temporal consistency, whereas the existing methods cannot. The mountain road scenes in the category of country contain many difficult cases to process such as missing lanes, illumination changes, and pitch angle variation as in the sixth row in Fig. 11. Although the detection result is less satisfactory than other scenes, our method still yields better performances than the existing methods. In fact, our method produced the highest detection rates for each of the four categories in the dataset.

The proposed algorithm yields satisfactory results with sharp curvature, lane changes, night roads, obstacles, and lens flares due to using the temporal consistency of lane width on each scanline. Although the positions of detected lane points are sometimes not exact when the width of the lane points abruptly changes in the spatiotemporal image due to abrupt pitch angle variation, our method still yields better detection rates than either Borkar's or Yoo's methods. The main reason for this is that most frame-based methods detect lanes or lane points over a whole frame and do not consider temporal consistency along the time axis.

Computational efficiency was also evaluated using our dataset. In the analysis of a 1-second video, the proposed method took 0.117 seconds, compared to 0.346 s for Borkar's method [9].

IV. Conclusion

In this paper, we have proposed an efficient algorithm for road lane detection based on spatiotemporal images. Lane points can be efficiently and effectively detected by aligning scanlines along the time axis and then applying a Hough transform. The positions of the detected lane points are used to calculate the predicted alignment offset of the scanline in the next frame. The detected lane points in each frame are fitted to a cubic curve. As a result, the proposed method using temporal consistency becomes robust to missing lanes, in particular. The experimental results demonstrated not only the superior computational efficiency of our algorithm but also its improved detection rates.

Acknowledgment

The authors would like to thank A. Borkar, M. Hayes, and M. T. Smith for dataset [9]. They also thank H. Yoo, U. Yang, and K. Sohn for providing their dataset [11] and binary codes.

References

[1] P. Y. Hsiao, C. W. Yeh, S. S. Huang, and L. C. Fu, "A portable vision based real-time lane departure warning system: Day and night," *IEEE Trans. Veh. Technol.*, vol. 58, no. 4, pp. 2089–2094, May 2009.
[2] J. P. Carrasco, A. de la Escalera, and J. M. Armingol, "Driving supervision through traffic sign analysis," in *Proc. IEEE Int. Conf. Veh. Electron. Safety*, Columbus, OH, USA, 2008, pp. 42–247.
[3] J. Deng, J. Kim, H. Sin, and Y. Han, "Fast lane detection based on the B-Spline fitting," *Int. J. Res. Eng. Technol.*, vol. 2, no. 4, pp. 134–137, 2013.
[4] O. Khalifa, A. Assidiq, and A. Hashim, "Vision-based lane detection for autonomous artificial intelligent vehicles," in *Proc. IEEE Int. Conf. Semantic Comput.*, 2009, pp. 636–641.
[5] J. Wang, Y. Wu, Z. Liang, and Y. Xi, "Lane detection based on random Hough transform on region of interesting," in *Proc. IEEE Conf. Inf. Autom.*, 2010, pp. 1735–1740.
[6] M. Aly, "Real time detection of lane markers in urban streets," in *Proc. IEEE Intell. Veh. Symp.*, Jun. 2008, pp. 7–12.
[7] Q. Chen and H. Wang, "A real-time lane detection algorithm based on a hyperbola-pair model," in *Proc. IEEE Intell. Veh. Symp.*, Jun. 2006, pp. 3–15.
[8] G. Y. Jiang, "Lane and obstacle detection based on fast inverse perspective mapping algorithm," in *Proc. IEEE Conf. Syst., Man Cybern.*, 2000, pp. 2969–2974.
[9] A. Borkar, M. Hayes, and M. T. Smith, "A novel lane detection system with efficient ground truth generation," *IEEE Trans. Intell. Transp. Syst.*, vol. 13, no. 1, pp. 365–374, Mar. 2012.
[10] Z. Kim, "Robust lane detection and tracking in challenging scenarios," *IEEE Trans. Intell. Transp. Syst.*, vol. 9, no. 1, pp. 16–26, Mar. 2008.
[11] H. Yoo, U. Yang, and K. Sohn, "Gradient-enhancing conversion for illumination-robust lane detection," *IEEE Trans. Intell. Transp. Syst.*, vol. 14, no. 3, pp. 1083–1094, Sep. 2013.
[12] U. Meis, W. Klein, and C. Wiedemann, "New method for robust far distance road course estimation in advanced driver assistance systems," in *Proc. IEEE Conf. Intell. Transp. Syst.*, 2010, pp. 1357–1362.
[13] J. McCall, D. Wipf, M. Trivedi, and B. Rao, "Lane change intent analysis using robust operators and sparse Bayesian learning," *IEEE Trans. Intell. Transp. Syst.*, vol. 8, no. 3, pp. 431–440, Sep. 2007.
[14] M. Bertozzi and A. Broggi, "Gold: A parallel real-time stereo vision system for generic obstacle and lane detection," *IEEE Trans. Image Process.*, vol. 7, no. 1, pp. 62–81, Jan. 1998.
[15] R. Aufrere, R. Chapuis, and F. Chausse, "Real time vision based road lane detection and tracking," in *Proc. MVA*, Tokyo, Japan, Nov. 2000, pp. 75–78.
[16] R. K. Satzoda and M. M. Trivedi, "Selective salient feature based lane analysis," in *Proc. IEEE Intell. Transp. Syst. Conf.*, 2013, pp. 1906–1911.
[17] T. Sun, S. Tsai, and V. Chan, "HSI color model based lane-marking detection," in *Proc. IEEE Intell. Transp. Syst. Conf.*, 2006, pp. 1168–1172.
[18] K. Chin and S. Lin, "Lane detection using color-based segmentation," in *Proc. IEEE Intell. Veh. Symp.*, 2005, pp. 706–711.

[19] R. Gopalan, T. Hong, M. Shneier, and R. Chellappa, "A learning approach towards detection and tracking of lane markings," *IEEE Trans. Intell. Transp. Syst.*, vol. 13, no. 3, pp. 1088–1098, Sep. 2012.

[20] E. D. Dickmanns and A. Zapp, "A curvature-based scheme for improving road vehicle guidance by computer vision," in *Proc. SPIE*, 1986, vol. 727, pp. 161–168.

[21] H. Loose, U. Franke, and C. Stiller, "Kalman particle filter for lane recognition on rural roads," in *Proc. IEEE Intell. Veh. Symp.*, Jun. 2009, pp. 60–65.

[22] N. Benmansour, R. Labayrade, D. Aubert, S. Glaser, and D. Gruyer, "A model driven 3D lane detection system using stereovision," in *Proc. Control, Autom., Robot. Vis.*, 2008, pp. 1277–1282.

[23] J. L. Barron, D. J. Fleet, and S. S. Beauchemin, "Performance of optical flow techniques," *Int. J. Comput. Vis.*, vol. 12, no. 1, pp. 43–77, Feb. 1994.

[24] E. H. Adelson and J. R. Bergen, "Spatiotemporal energy models for the perception of motion," *J. Opt. Soc. Amer. A, Opt. Image Sci.*, vol. 2, no. 2, pp. 284–299, Feb. 1985.

[25] H. Kim, J. Lee, J. Yang, S. Sull, and S. M. Song, "Visual rhythm and shot verification," *Multimedia Tools Appl.*, vol. 15, no. 3, pp. 227–245, Dec. 2001.

[26] T. A. Smadi, "Real-time lane detection for driver assistance system," *J. Circuits Syst.*, vol. 5, no. 8, pp. 201–207, May. 2014.

[27] J. Son, H. Yoo, S. Kim, and K. Sohn, "Real-time illumination invariant lane detection for lane departure warning system," *Expert Syst. Appl.*, vol. 42, no. 4, pp. 1816–1824, Mar. 2015.

[28] Y.-Z. Peng and H.-F. Gao, "Lane detection method of statistical Hough transform based on gradient constraint," *Int. J. Intell. Inf. Syst.*, vol. 4, no. 2, pp. 40–45, Mar. 2015.